


## Research Article

# A Low-Cost Wideband Digital Array Antenna Based on Stretch Processing Technique

Daqun Yu <sup>1,2</sup>, Zhangcheng Hao,<sup>1</sup> Lei Yang,<sup>2</sup> Yang Wang,<sup>2</sup> Lei Sun,<sup>2</sup> and Jianjun Mao<sup>2</sup>

<sup>1</sup>School of Information Science and Engineering, Southeast University, Nanjing 210096, China

<sup>2</sup>Nanjing Research Institute of Electronics Technology, Nanjing 210039, China

Correspondence should be addressed to Daqun Yu; [yulipii@163.com](mailto:yulipii@163.com)

Received 2 December 2023; Revised 6 April 2024; Accepted 8 April 2024; Published 24 April 2024

Academic Editor: Trushit Upadhyaya

Copyright © 2024 Daqun Yu et al. This is an open access article distributed under the Creative Commons Attribution License, which permits unrestricted use, distribution, and reproduction in any medium, provided the original work is properly cited.

Wideband digital phased array radar offers the advantages of high range resolution, which improves the recognition ability for multiple targets, group targets, and high-speed targets. Traditional wideband phased arrays use true time delay to compensate for aperture fill time; however, the cost increases significantly. In this paper, a wideband elemental digital array architecture based on the stretch processing method is proposed. By utilizing the time-domain and frequency-domain translation equivalence of the LFM (Linear Frequency Modulation) signal waveform, the equivalent aperture fill time is compensated for through frequency shift and phase shift after stretch processing. Compared to traditional wideband digital arrays, this method can dramatically reduce the required sampling rate and lower the requirements on antenna hardware, thereby reducing the manufacturing cost of system. A comprehensive analysis of the signal processing process and stretch processing method is provided. And an antenna array prototype is developed to verify the T/R channel compensation and wideband beamforming. Measured results show that the antenna is capable of  $\pm 60^\circ$  scanning in azimuth plane and  $\pm 40^\circ$  scanning in elevation plane, with a bandwidth of 500 MHz in S-band. The results demonstrate excellent wideband beam performance and accurate lobe scanning, which confirms the validity of the proposed wideband architecture for stretch processing, frequency shift, and phase shift. This method can be widely applied to the low-cost design and wideband performance improvement of wideband digital array radar.

## 1. Introduction

Wideband phased array radar offers significant performance advantages and is considered as crucial defense equipment which has been highly valued by various countries. Compared to narrowband phased array radars, wideband phased array radars obtain great improvements in range resolution, which will raise the radar performance in target classification and identification [1–4]. The wideband phased array antenna system is the core component of wideband phased array radar. For a wideband phased array antenna system, when the antenna aperture and signal bandwidth increase, the aperture effect worsens, resulting in energy loss and waveform distortion of the echo signal, and thus the radar's coverage evaluation decreases [5]. Therefore, compensating for aperture fill time is significant in achieving wideband performance in phased array antennas.

For the analog active phased array antenna system, time delay is usually realized by real-time delay lines in the form of RF or optical fiber [6]. Wideband analog active phased array antennas often employ subarray level time delay design to reduce costs, bulk, and weight. However, this approach will result in a decrease in instantaneous bandwidth and higher subarray quantization lobes [7–9] in the wideband antenna pattern, as shown in Figure 1. In contrast, time delay in digital phased array antenna systems is realized by digital signal processing. Digital delay compensation [10, 11] is achieved through FPGA (Field Programmable Gate Array), DSP (Digital Signal Processor), DAC (Digital to Analog Converter), ADC (Analog to Digital Converter), and other digital hardware, as well as wideband digital signal processing algorithms. These high-speed digital devices are expensive, and sampling large amounts of data at high speeds leads to difficulties in data transmission and

processing. Especially, for radar systems with multiple receive channels, the data rate can exceed the processing capacity of the signal processing [12]. Both analog and digital wideband phased array radars always result in a significant increase in cost. Therefore, a low-cost, high-performance wideband phased array radar is of great engineering importance.

Linear Frequency Modulation (LFM) signals are one of the most common signal forms used in wideband phased array radar. After time delay, the LFM signal can be equivalent as a LFM signal with certain frequency shift and phase shift. Based on the characteristics, the stretch processing method [13, 14] has been developed to convert wideband signals into narrowband signals through frequency-time conversion. The received signal is stretched by mixing it with a local oscillator LFM signal that has the same frequency modulation (FM) slope as the transmitted signal. After the mixing operation, targets at different ranges appear at distinct frequencies. This method significantly reduces the sampling rate of the ADC and the production cost.

The stretch method was first successfully applied to the U.S. range measurement radar ALCOR [15, 16], which operates in C-band. It has a signal instantaneous bandwidth of 500 MHz and a time width of 10  $\mu$ s. Using the stretch method, the time delay only needs to be implemented in the video, which significantly reduces the design requirements of the complex feeder network and the cost of expensive ADCs, DACs, and other devices. In recent years, researchers have been exploring the theoretical analysis and engineering practice of the stretch method. De-ping et al. [17] investigated transmitting digital beamforming based on Direct Digital Synthesis (DDS). Liu Haibo et al. [18] discussed the theory related to the wideband LFM stretching process in detail and conducted a 600 MHz wideband LFM signal stretching test using 8 transmit channels and 8 receive channels based on digital T/R components. However, in previous research, there have been few studies on the low-cost engineering implementation of a fully digital wideband antenna array system [19]. Literature [20] raises a novel subarray digital modulation technique for wideband phased array radar, but the stretch processing is realized in digital domain and many high-speed ADCs are used, for which it is difficult to reduce cost. A high-resolution on-chip S-band radar system using stretch processing was developed in [21, 22]. In this system, the bandwidth of the signal could exceed 600 MHz to provide high resolution, and the sampling rate of ADCs is dramatically reduced by the usage of stretch processing. But the detailed architecture of the antenna array is not introduced. Venere et al. [23] proposed a receiver circuit with low cost and low power consumption that employs stretch processing. The cost is reduced from the perspective of device optimization rather than the antenna array architecture. The authors of [24, 25] proposed the improvement of signal processing algorithms for stretch processing in synthetic aperture radar (SAR) and multiple-input multiple-output (MIMO) radar systems.

This paper proposes a wideband digital array antenna at the element level, utilizing the stretch processing method to integrate wideband signal capability into the digital array

antenna system. In this system, wideband signals that each radiating unit transmits and receives are stretched before digitization. This stretching greatly reduces the sampling rate of the ADC and eliminates the need to increase the number of time-delay modules. As a result, the system has a simple hardware implementation and low fabrication cost and exhibits good performance in terms of wideband antenna pattern. In this paper, a prototype of an elemental digital array antenna was fabricated and tested to demonstrate the validity of the proposed approach. The transceiver/receiver channel calibration has been completed, and the wideband pattern has been tested. Experimental data show that the prototype has excellent performance and can be applied to a wideband digital array radar system, which is of great significance for reducing the manufacturing cost of wideband radar systems.

## 2. Stretch Processing Principle

*2.1. Stretch Processing Method.* The stretch processing method for wideband LFM signal was first proposed by Caputi [15]. When the target echo arrives, the receiver generates a local oscillator (LO) signal with the same frequency modulation slope as the received signal. Then, after the mixing process, the target echo becomes a signal whose frequency is proportional to the echo arrival time. Figure 2 shows the schematic diagram illustrating the principle of processing wideband radar signals using the time-frequency conversion method.

As shown in Figure 2(a), the LFM signal generated by the digital approach has a time width  $T$ , a bandwidth  $B$ , and an initial frequency  $f_{\text{start}}$ . The time-bandwidth product of the linear FM signal is derived as  $B \cdot T$ . The signal satisfies the relation:

$$f = f_{\text{start}} + kt = f_{\text{start}} + \frac{B}{T}t, \quad (1)$$

where  $k = B/T$  represents the FM slope (pulse compression ratio). As shown in Figure 2(b), the echo signals from different parts of the target are depicted by solid lines. The horizontal translation of these lines represents the different arrival times of the echoes, with the head echo arriving first and the tail echo arriving last. The dotted line represents the principal oscillator signal of the receiving channel, whose FM slope should be the same as that of the transmitting signal. In this paper, a low local oscillator is used, meaning that the frequency of the local oscillator signal is lower than the frequency of the transmit signal. The center frequency of the local oscillator signal is  $f_{\text{LO}}$ . Therefore, there is a relation equation:

$$f_{\text{start}} = f_{\text{IF}} - \frac{B}{2} + f_{\text{LO}}. \quad (2)$$

As shown in Figure 2(c), the echo signals are mixed with the stretched local oscillator signals to obtain the IF signals  $f_{\text{IF}}$ . The IF signal of each echo is a single carrier frequency signal, which has varying frequencies based on the arrival times of the echoes. The IF frequency of the first arriving echo is low, while that of the later arriving echo is high. Therefore, the time delay relationship of the echo signal can be converted into a frequency relationship after stretching.

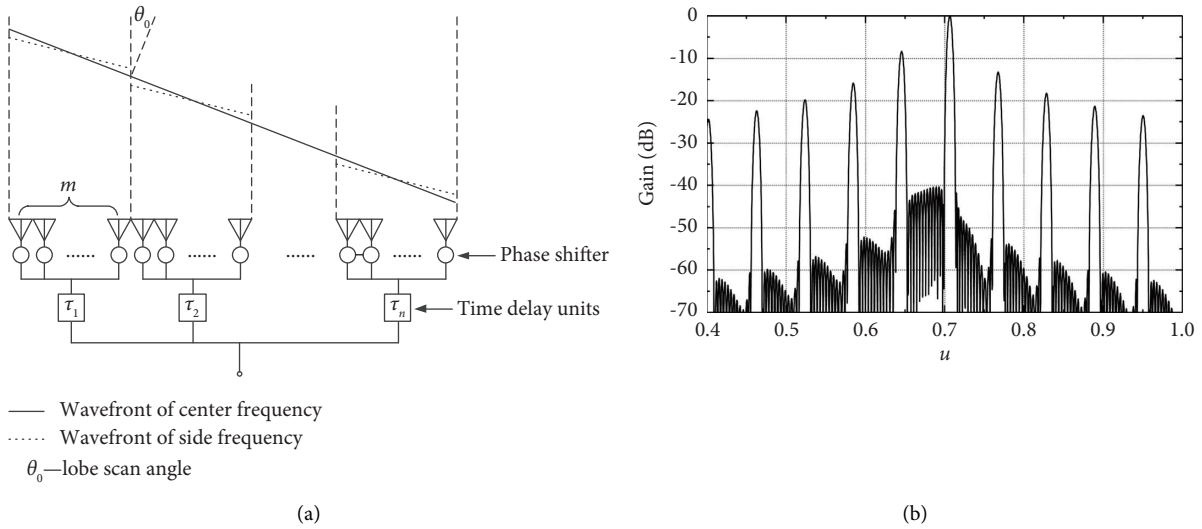


FIGURE 1: Scanning quantization lobe of subarray level time delay radar [7] (subarray number  $n = 16$ , element number in a subarray  $m = 32$ , and scanning angle  $\theta_0 = 45^\circ$ , with  $-40$  dB Taylor weight). (a) Array model. (b) Antenna array pattern.

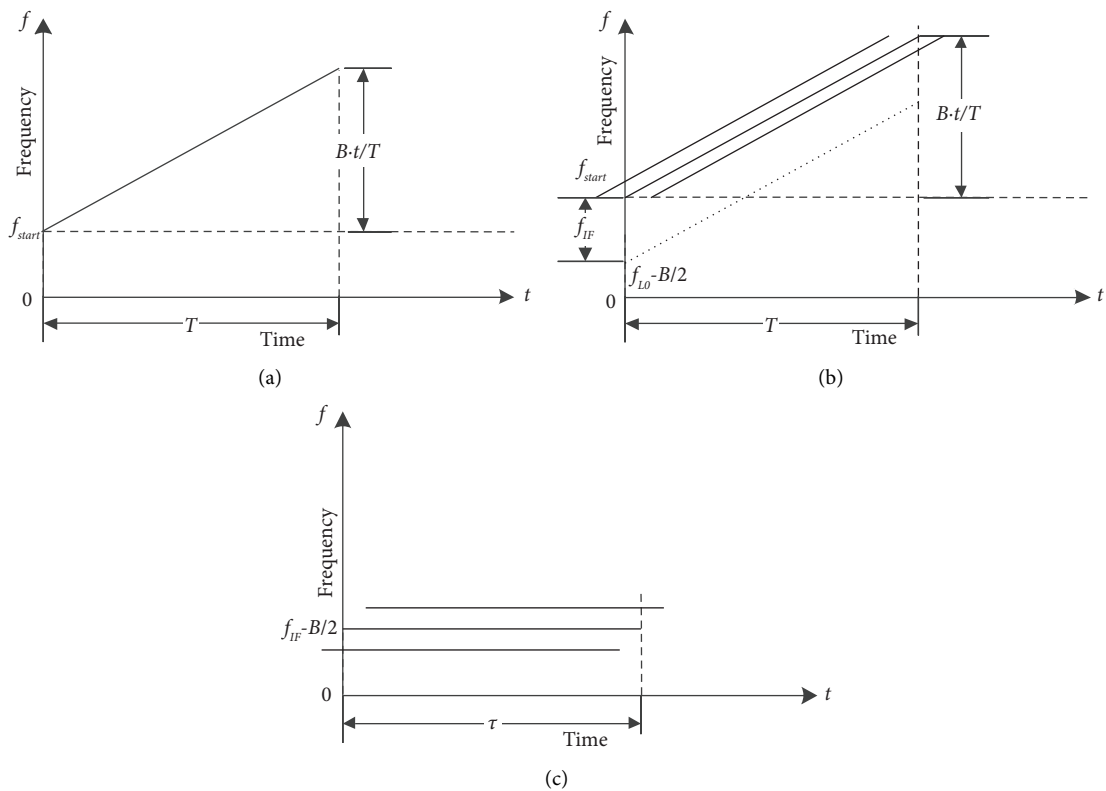


FIGURE 2: Relationship between signal frequency and time. (a) Transmitted signal. (b) Received signal. (c) Stretched signal.

**2.2. Stretch Processing in Elemental Digital Wideband Array Antenna.** The elemental wideband digital array based on the stretch processing method proposed in this paper, compared with the narrowband digital phased array system, aims to achieve wideband operation. It only requires the frequency source to output the wideband LFM local oscillator signal. Additionally, the amplification, frequency conversion, and

sampling parts can still be directly used for narrowband digital sampling. The antenna system design focuses on the stretch processing algorithm. The original narrowband digital antenna array can achieve wideband capability through a simple software update, significantly reducing the cost of expanding the bandwidth. Using the wideband frequency shift and phase shift method proposed in Section

3 of this paper, it is possible to achieve accurate compensation of the wideband beam aperture fill time.

The basic components of an elemental digital array radar are shown in Figure 3. The digital components are digitized at the element level, and each antenna element is individually connected to an excitation source and a receiver. The Direct Digital Synthesis (DDS) of each transmitting channel generates excitation signal based on the control signal. The Analog-to-Digital Converter (ADC) of each receiving channel receives the signal and digitizes it. Digital Beamforming (DBF) is used to simultaneously form multiple independently directed digital beams, eliminating the need for analog phase shifters and beam synthesis networks.

When the antenna array works in wideband operation, the local oscillator outputs a wideband LFM signal, which is mixed with the wideband echo signal and results in a significant reduction in the signal bandwidth. Therefore, it can be multiplexed with narrowband digital transceiver channels. This wideband operation requires beam synthesis through the control of the frequency and phase of the IF signal.

The digital T/R component is an important part of this antenna system, and its internal composition is shown in Figure 4. The digital channel mainly consists of FPGA, DDS, ADC, and other components. The number of bits in the DDS and ADC directly determines the accuracy of frequency shift and phase shift, which in turn affects the wideband performance of the antenna array. The DDS frequency shift accuracy of the digital T/R components designed in this paper is quantized to 32 bits, with a minimum shift of 0.0279 Hz. The phase shift accuracy is quantized to 16 bits with a minimum shift of 0.0055°.

It is worth noting that, when stretch operation is performed for the elemental digital array antenna, alignment between transmission signal, echo signal, and wideband local oscillator signal is crucial. Besides, the channel delay and in-band characteristics need to be calibrated to ensure the array performance. The stretch processing method is only effective for the wideband linear frequency modulation signal but not applicable for other forms of wideband waveforms.

### 3. Wideband Beam Scanning

Based on the hardware architecture mentioned above, the implementation of aperture fill time compensation algorithms is necessary for wideband beam scanning using LFM signals. As shown in Figure 2, the delay of the wideband LFM signal in the time domain can be equivalent as frequency and phase changes of this signal in the frequency domain. Therefore, compensating for time delay can be achieved by adjusting the frequency and phase. In this chapter, the principle of wideband beam scanning is fully deduced. The block diagram of this principle is shown in Figure 5. The elemental digital array antenna is designed for pulse radar system, in which the transmitting and receiving channels do not work at the same time. The circulator between transmitting and receiving sides can provide isolation of better than 20 dB.

**3.1. Wideband Transmit Beam.** The principle of wideband transmit beam formation is shown in Figure 5(a). A local oscillator signal generated by the frequency source is in the following form:

$$S_{LO}(t) = \cos\left\{2\pi\left[\left(f_{LO} - \frac{B}{2}\right)t + \frac{1}{2}(kt^2)\right]\right\} \cdot \text{rect}\left(\frac{t - (T/2)}{T}\right), \quad (3)$$

$$\text{rect}\left(\frac{t - (T/2)}{T}\right) = \begin{cases} 1, & 0 < t < T, \\ 0, & \text{others.} \end{cases} \quad (4)$$

When the antenna array radiates energy at an angle of  $\theta$  away from the normal of the array plane, the arrangement of each element causes a different distance between each element and the same location in space. To ensure that each antenna signal is superimposed in the same phase at the same location in space, it is necessary to delay the signals of different elements to compensate for the wavelength difference caused by the antenna beam pointing away from the normal. Taking the 1<sup>st</sup> antenna element as a reference, the  $(i + 1)$ <sup>th</sup> antenna element transmits a signal of the form:

$$S(t - \tau_i) = \cos\left\{2\pi\left[f_{\text{start}}(t - \tau_i) + \frac{k(t - \tau_i)^2}{2}\right]\right\} \cdot \text{rect}\left(\frac{t - (T/2)}{T}\right), \quad (5)$$

where the relationship between the starting frequency  $f_{\text{start}}$  of the transmit signal and the intermediate frequency signal  $f_{IF}$  satisfies (2) and

$$\tau_i = \frac{i \cdot d \cdot \sin \theta}{c}, \quad (6)$$

where  $d$  is the spacing between antenna array elements. The above equation ignores the effect of the envelope term since  $\tau_i$  is much smaller than  $T$ . According to the principle shown in Figure 2, the transmitting signal is obtained by mixing the IF signal with the local oscillator signal. Therefore, the IF transmitting signal that needs to be generated for the  $(i + 1)$ <sup>th</sup> element is

$$S_{IF_{i+1}}(t) = \cos\left\{2\pi\left[\left(f_{IF} - k\tau_i\right)t + \frac{k\tau_i^2}{2} - f_{\text{start}} \cdot \tau_i\right]\right\} \cdot \text{rect}\left(\frac{t - (T/2)}{T}\right). \quad (7)$$

That is, the signal represented by (3) is mixed with the signal represented by (7) to obtain (5). From the coefficients of  $t$  in (7), the frequency bias of the IF signal generated by the  $(i + 1)$ <sup>th</sup> DDS is calculated using the 1<sup>st</sup> channel as a reference:

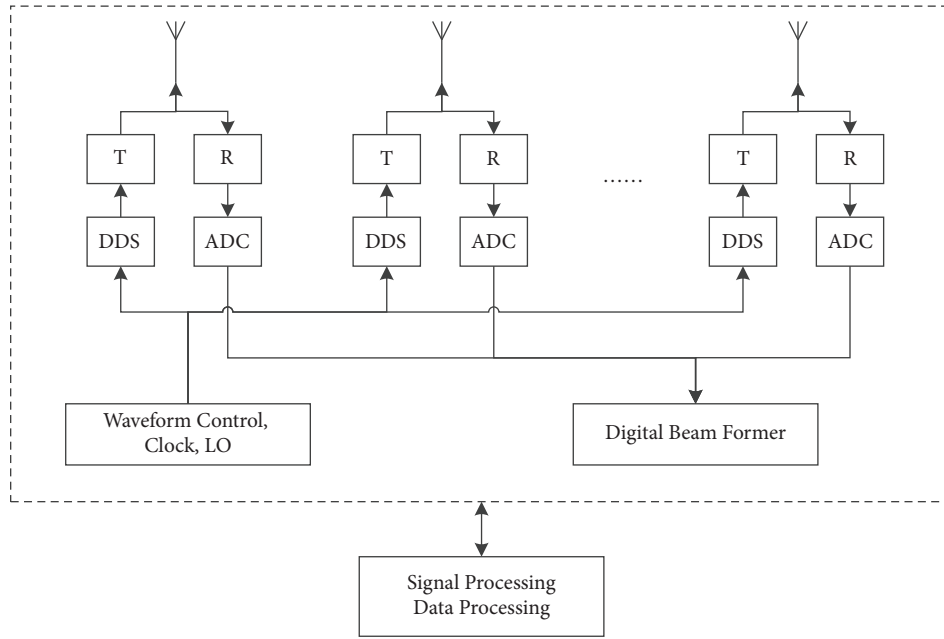


FIGURE 3: Diagram of elemental digital array antenna.

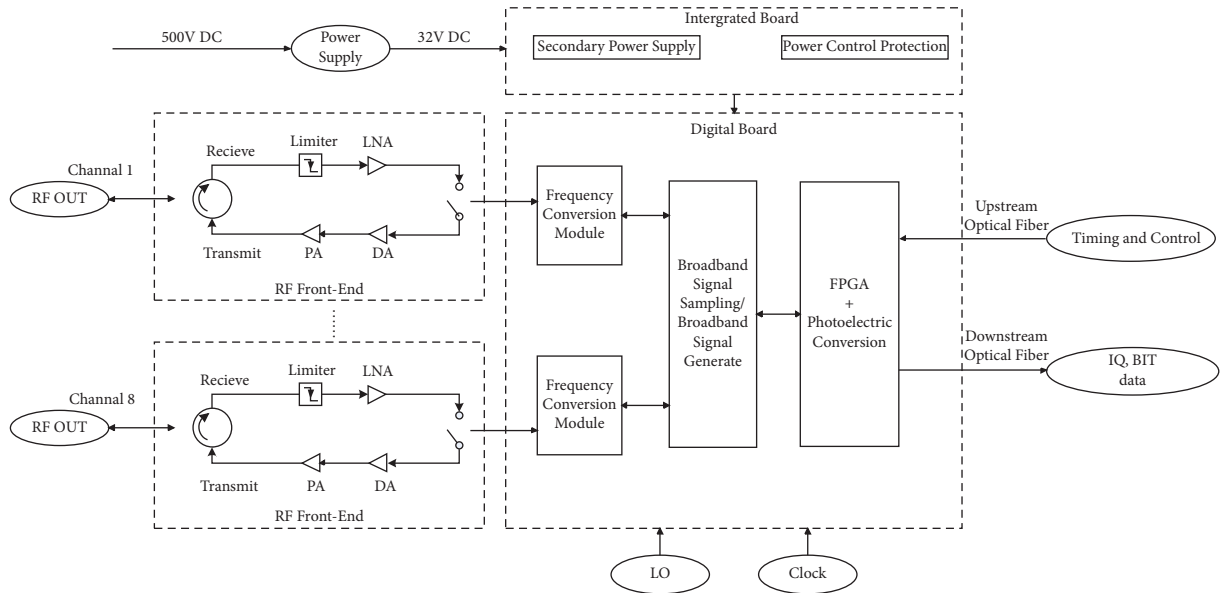


FIGURE 4: Diagram of digital T/R module.

$$\Delta f = k\tau_i = \frac{k \cdot i \cdot d \cdot \sin \theta}{c} \quad (8)$$

The phase value of the IF signal generated by the  $(i+1)^{\text{th}}$  DDS is

$$\Delta \varphi = 2\pi \left[ \frac{k\tau_i^2}{2} - f_{\text{start}}\tau_i \right] \quad (9)$$

Based on the results of the calculations of (8) and (9), the required frequency shift and phase shift values for each element in the array corresponding to the wideband beam scan can be obtained.

**3.2. Wideband Receive Beam.** The reception of instantaneous wideband signal processing flow is shown in Figure 5(b). The digital reception part includes functions such as frequency shift and phase shift, digital delay, and so on. When the LFM signal is received, the local oscillator network assigns the stretched local oscillator signal with wideband LFM characteristics to each receiving channel for mixing. The resulting mixed IF signal is then sampled by the ADC and sent to the FPGA for processing.

Assuming that a target exists at a distance  $R$ , the target echo signal received by the  $(i+1)^{\text{th}}$  antenna unit is

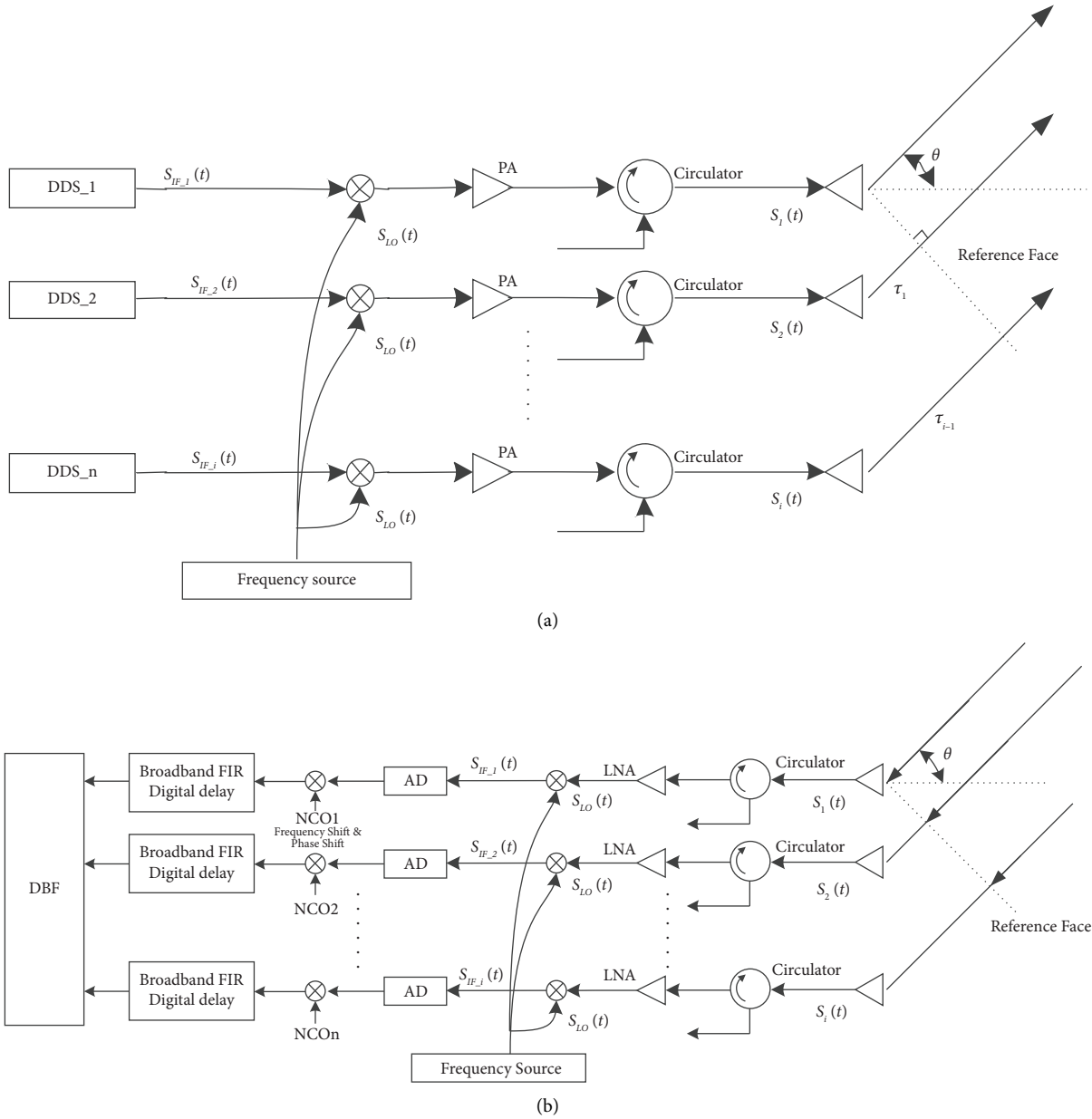


FIGURE 5: Diagram of beam scanning for elemental wideband digital array antenna. (a) Transmit. (b) Receive.

$$S(t - a_i) = \cos \left\{ 2\pi \left[ f_{\text{start}}(t - a_i) + \frac{1}{2}k(t - a_i)^2 \right] \right\} \cdot \text{rect} \left( \frac{t - a_i - (T/2)}{T} \right), \quad (10)$$

where

$$\begin{cases} \alpha_i = \Delta + \tau_i, \\ \Delta = \frac{2R}{c}, \end{cases} \quad (11)$$

where  $\alpha_i$  represents the return delay time of the  $(i + 1)^{\text{th}}$  unit and  $\Delta$  represents the delay time from the equivalent phase center of the antenna array to the target, and this value is not dependent on the element number.  $\tau_i$  is calculated in the

same way as in (6), and  $\beta_i$  is independent of the target distance and is only related to the beam pointing, cell spacing, and the unit position, as shown in Figure 6.

The frequency source generates a stretched local oscillator signal in the following form:

$$S_{\text{LO}}(t) = \cos \left\{ 2\pi \left[ \left( f_{\text{LO}} - \frac{B}{2} \right) t + \frac{1}{2}kt^2 \right] \right\} \cdot \text{rect} \left( \frac{t - (T_{\text{ref}}/2)}{T_{\text{ref}}} \right), \quad (12)$$

where  $T_{\text{ref}}$  is the pulse width of the stretched local oscillator signal (usually  $T_{\text{ref}} > T$ ). The return signal (10) is mixed with the stretched local oscillator (12) and then passed through a low-pass filter to obtain an IF signal.

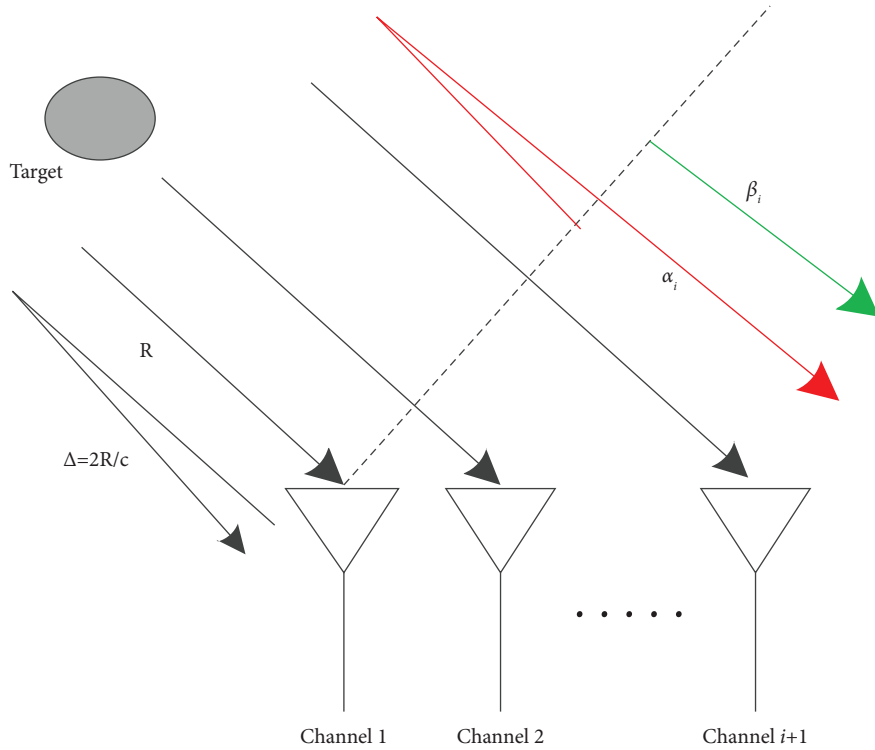


FIGURE 6: Schematic diagram of echo time delay.

$$S_{\text{IF}_i}(t) = \cos\{2\pi[f_{\text{IF}}t + k(\tau_r - \alpha_i)t + \phi(\alpha_i)]\} \cdot \text{rect}\left(\frac{t - \alpha_i - (T/2)}{t}\right) \cdot \text{rect}\left(\frac{t - (T_{\text{ref}}/2)}{T_{\text{ref}}}\right), \quad (13)$$

where

$$\phi(\alpha_i) = -\Delta \cdot f_{\text{start}} + \frac{k}{2}\Delta^2 + \frac{k}{2}\tau_i^2 - \tau_i \cdot f_{\text{start}} + k \cdot \Delta \cdot \tau_i. \quad (14)$$

The IF phase of each unit is shown in the equation above. The first two terms are independent of the unit number and are public quantities, while the last three terms are related to the unit number  $i$ . The third term is a small second-order quantity, which can be estimated to be on the order of  $10^{-2}$  degrees based on the maximum FM slope. Therefore, it can be disregarded. Up to this point, the echo signal is mixed with the local oscillator to complete the stretched operation, and the coefficient of  $t$  in (13) represents the IF frequency of each unit.

As can be seen from (13) and (14), the frequency and phase of the IF signal of each unit are related to the position (or number) of the channel. To ensure that the reception signals from each unit can be superposed in a coherent frequency and phase, the Numerically Controlled Oscillator (NCO) signals of the channel should be preset to the corresponding frequency and initial phase. Since it is difficult to accurately estimate the delay between the return signal and the opening time of the receiving gate, the starting frequency

of the reference channel for the NCO signal is typically set to  $f_{\text{IF}}$ . The NCO signal for the  $(i+1)^{\text{th}}$  channel should be

$$S_{\text{NCO}}(t) = \cos\{2\pi[f_{\text{IF}}t + k \cdot \tau_i \cdot t - f_{\text{start}} \cdot \tau_i + k \cdot \Delta \cdot \tau_i]\} \cdot \text{rect}\left(\frac{t - \alpha_i - (T_{\text{ref}}/2)}{T_{\text{ref}}}\right). \quad (15)$$

After mixing with the IF signal (13) and low-pass filtering, ignoring the minima and the common, the signal (IQ) is obtained and expressed as follows:

$$S_{\text{IQ-ini}} = \cos\{2\pi[\Delta \cdot kt + k \cdot \Delta \cdot \tau_i]\} \cdot \text{rect}\left(\frac{t - \alpha_i - (T/2)}{T}\right) \cdot \text{rect}\left(\frac{t - (T_{\text{ref}}/2)}{T_{\text{ref}}}\right). \quad (16)$$

The frequency and phase of this signal are  $\Delta \cdot k$  and  $k \cdot \Delta \cdot \tau_i$ , respectively. The phase can be seen as a residual amount of phase that occurs in the aperture crossing due to the remaining frequency resulting from the misalignment of the receiving gate with the return signal. It only varies with the channel number. This quantity can be eliminated by implementing a digital delay for each element, where the digital time delay for each channel is denoted as  $\tau_i$ . After frequency shifting, phase shifting, and delay processing, the signals from each element are completely synchronized in terms of frequency and phase, allowing for coherent synthesis. The delay can be ignored when the wideband operates with accurate guidance.

TABLE 1: Comparison of sampling rate and data transmission rate.

	Traditional wideband digital array	Wideband digital array with stretch processing
Bandwidth (MHz)	500	40
Sampling rate (MHz)	1200	120
ADC bits	14	16
Data transmission rate per digital channel (Gbps)	42 (1200 Mbps $\times$ 2 $\times$ 14/0.8)	4.8 (120 Mbps $\times$ 2 $\times$ 16/0.8)

#### 4. Analysis of Antenna Array Cost

After stretch processing of wideband signal to narrowband, the hardware requirements of analog-to-digital sample rate, FPGA processing, and sample data transmission have been reduced significantly. The LFM signal of 500 MHz is transformed to be less than 40 MHz. According to the Nyquist sampling theorem, the rate of sampling clock is reduced from 1.2 GHz to 120 MHz together with the requirements for data transmission rate, FPGAs, and multi-channel signal synchronization. The comparison is shown in Table 1.

For the eight-channel digital T/R module, the data transmission rate is reduced from 336 Gbps to 38.4 Gbps. Tables 2 and 3 show the comparison of cost for wideband digital T/R module and narrowband digital T/R module with stretch processing. After stretch processing, the cost is greatly reduced over 75%.

#### 5. Example

In this paper, a S-band prototype of low-cost elemental wideband digital array antenna is designed and measured, which is shown in Figure 7. The antenna prototype adopts an elemental digitized architecture, as shown in Figures 3 and 4. The type of radiating elements employed is patch antenna with the characteristics of wideband, wide-angle-scanning, and low-profile [26–28]. The prototype consists of 12 rows and 24 columns, with a total of 288 T/R channels.

The test bench block of the antenna system is illustrated in Figure 8. The antenna beams are realized by a digital beamforming (DBF) board. The measurements involve two main tasks [29]: the calibration of each antenna element and the measurement of the radiation pattern of the array.

The amplitude, phase, and time delay consistency of each channel after calibration are shown in Figure 9. The channel numbers in the figure are numbered as follows: in the case of the back view, the lower-left unit is element 1, and the numbering is carried out sequentially from bottom to top and from left to right. The amplitude and phase distribution of each element after compensation does not exhibit obvious steps or slopes and is randomly distributed. The remaining error is a systematic random error. As shown in Figure 9(a), the transmitting channel has an amplitude standard deviation of 0.99 dB and a phase standard deviation of 3.46° because the amplitude is not compensated. In Figure 9(b), the receiving channel has an amplitude standard deviation of 0.49 dB and a phase standard deviation of 3.33°. As shown in Figures 9(c) and 9(d), the residual delays of both the transmitting and receiving channels are subtracted from

their averaged values. The standard deviations of their relative delay amounts are 37.05 ps and 33.03 ps, respectively. These values are then converted to frequency deviations of 18.525 Hz and 16.515 Hz, which are very close to the frequency shift accuracy. The in-band curves of several channels are depicted in Figure 10, and the linearity of the amplitude-phase characteristics within the band is satisfactory. This consistency is also observed across all channels.

After compensating for consistency, the antenna system can be tested using far-field wideband scanning measurements. In this paper, the far-field pattern test method is the electronically controlled scanning method. This method involves controlling the antenna array to shift the frequency and phase to achieve wideband beam scanning. The beam signals of different pointing are recorded to draw a wideband pattern.

The wideband pattern performance of the prototype was tested using this method. The transmitted wideband beam was confirmed to have been synthesized properly by comparing the accuracy and coincidence of the beam pointing. The pattern diagrams are plotted as shown in Figure 11, which demonstrate the directional diagrams of normal, azimuth 60° scan, and elevation 40° scan during reception and transmission, respectively. To investigate the wideband beam focusing characteristics, this paper divided the received time-domain IQ signal into five copies during the experimental process. Each copy of the received signal at different angles was then converted to the frequency domain using pulse compression process, and amplitude of the peak was extracted. Based on the characteristics of the LFM signal, the processed data can be expressed as patterns in five different frequency bands (ranging from low to high), represented by F1 to F5. To demonstrate the absence of quantization effect, the array is operated with a –30 dB Taylor taper distribution in both the elevation and azimuth directions during reception. As shown in Figure 11, the wideband transceiver patterns achieve correct beam pointing in both the azimuth and elevation planes. The maximum transceiver pointing error is 0.04° in the azimuth 60° scan and 0.03° in the elevation 40° scan. In addition, there is no quantization lobe in the pattern, and the residual error has a lesser effect on the deterioration of the side lobe level. The pattern gain degradation is less than 4 dB in 60° scan, which mostly originates from the characteristics of radiating elements. The results prove that the wideband beam achieves accurate synthesis, which is consistent with the theoretical derivation presented in this paper.

It is worth noting that the residual time delay in (16) has been ignored in the above pattern measurement. Since the target distance in the experiment is slightly larger than the



TABLE 2: Cost of an eight-channel wideband digital T/R module.

Device	Model	Price (RMB)	Quantity	Total (RMB)	Manufacturer
ADC	AD9680BCPZ-1250 (2-channel)	3000	4	120000	ADI
DAC	AD9154BCPZRL (4-channel)	500	2	1000	ADI
FPGA	XC7VX690T	6000	1	6000	Xilinx
Clock management chip	HMC7043LP7FE	80	1	80	ADI
40G QSFP + light module	TR-QQ85X-N00	100	9	900	InnoLight
Total				19980	

TABLE 3: Cost of 8-channel narrowband digital T/R module with stretch processing.

Device	Model	Price (RMB)	Quantity	Total (RMB)	Manufacturer
ADC	AD9268BCPZ-125 (2-channel)	800	4	3200	ADI
DAC	AD9959BCPZ (4-channel)	300	2	600	ADI
FPGA	XC7K325T	700	1	700	Xilinx
Clock management	Not needed				
40G QSFP + light module	TR-QQ85X-N00	100	1	100	InnoLight
Total				4600	

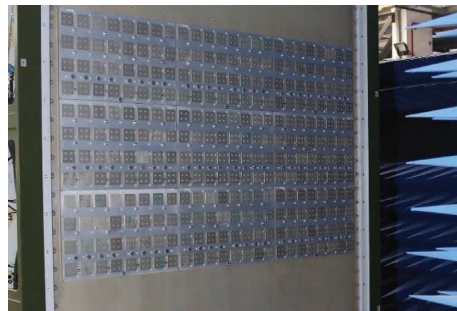


FIGURE 7: Photo of the prototype of the wideband digital array antenna in microwave anechoic chamber.

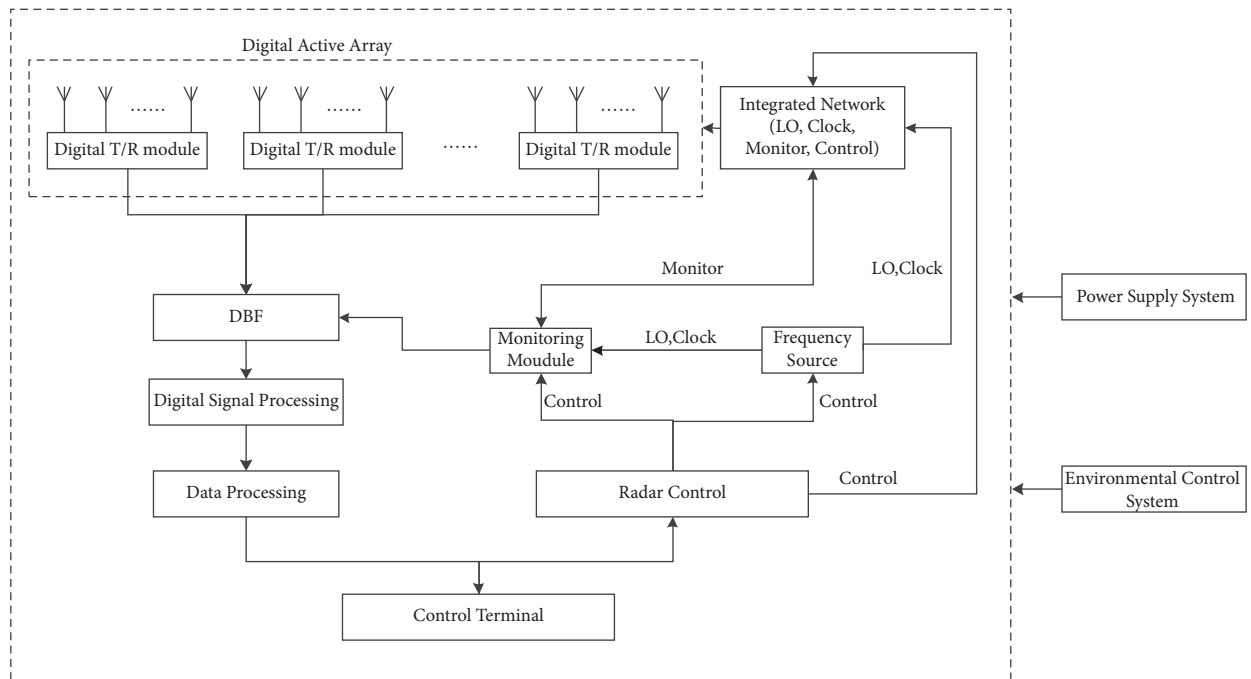


FIGURE 8: Diagram of the test bench for the prototype.

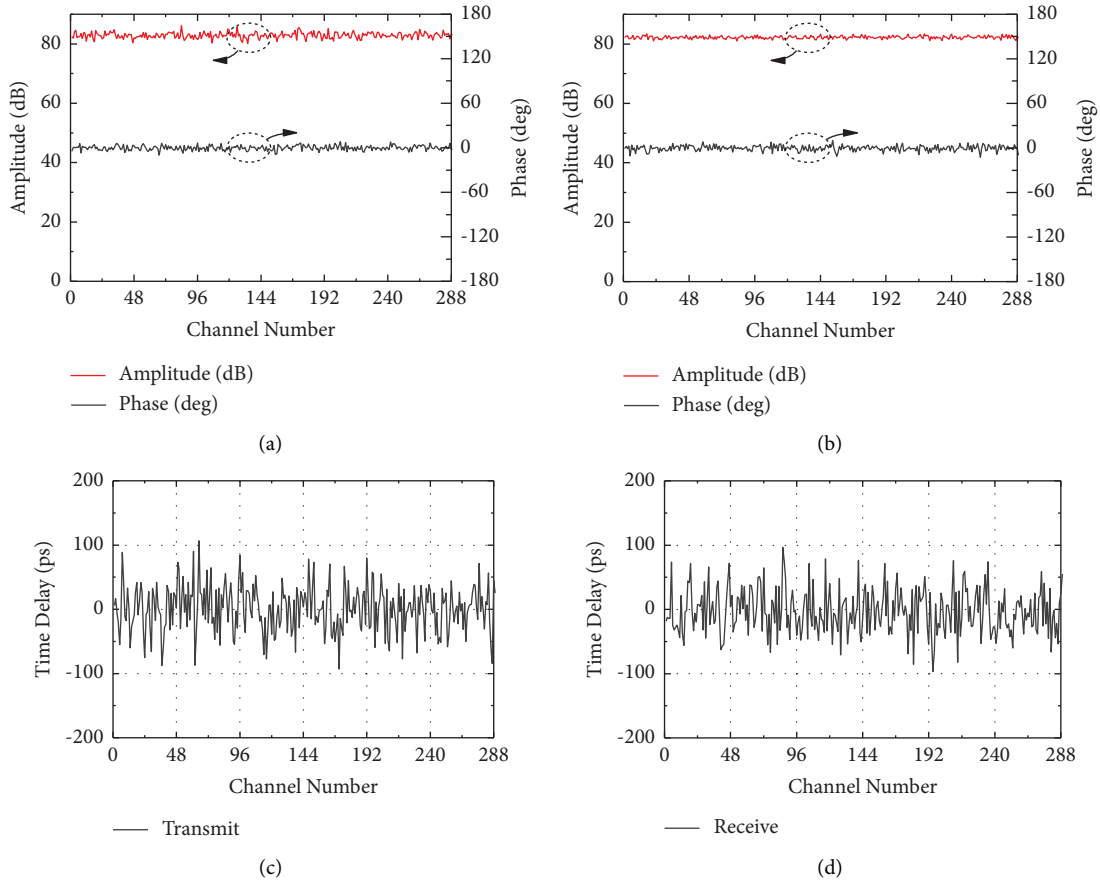


FIGURE 9: Measured results of channel consistency after compensation. (a) Transmit amplitude/phase. (b) Receive amplitude/phase. (c) Transmit time delay. (d) Receive time delay.

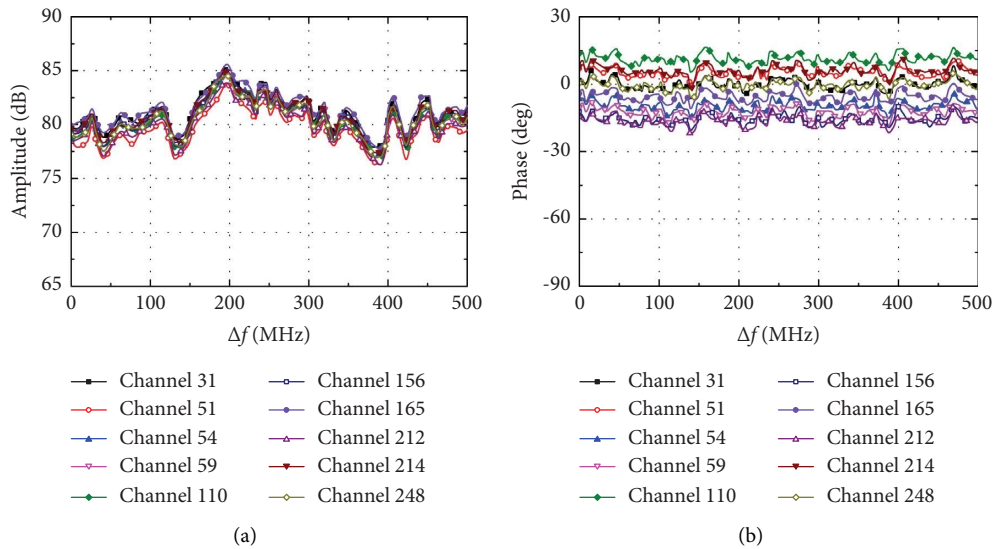


FIGURE 10: Continued.

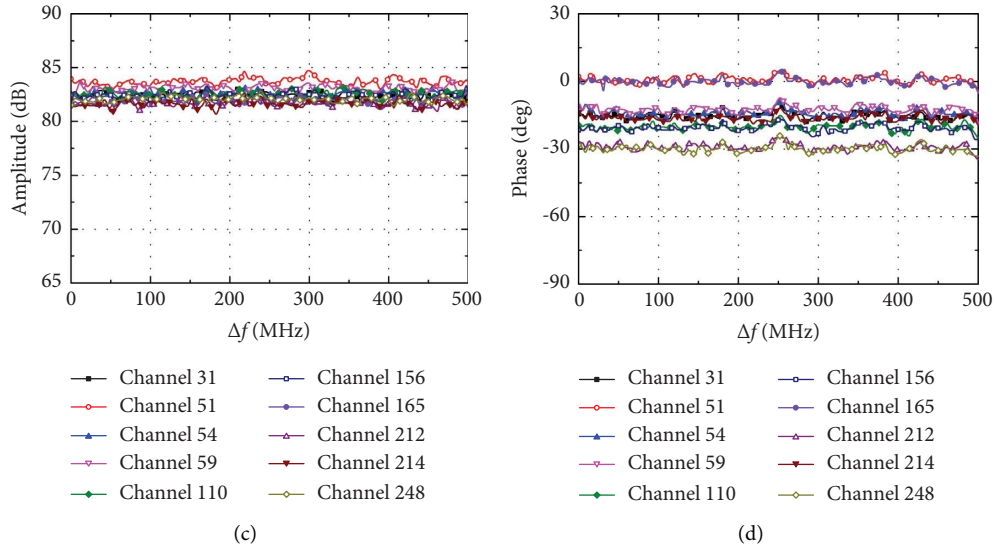


FIGURE 10: Measured results of in-band curve after compensation. (a) Transmit amplitude. (b) Transmit phase. (c) Receive amplitude. (d) Receive phase.

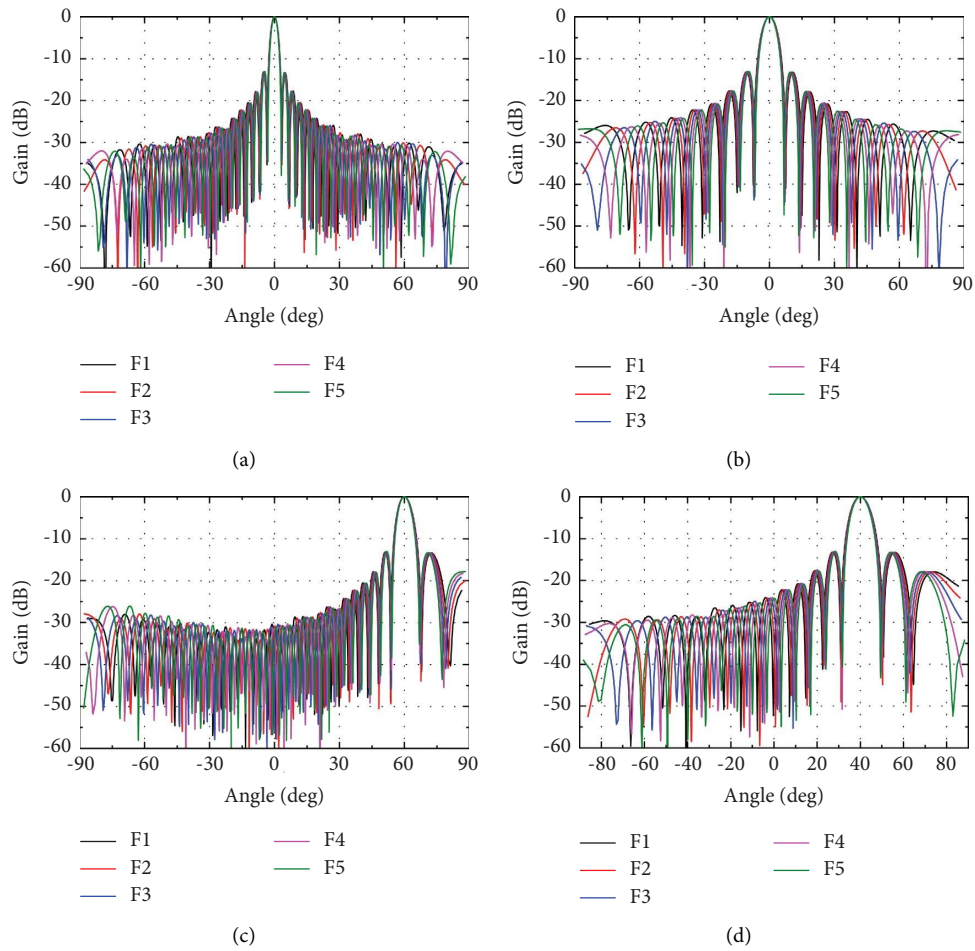


FIGURE 11: Continued.

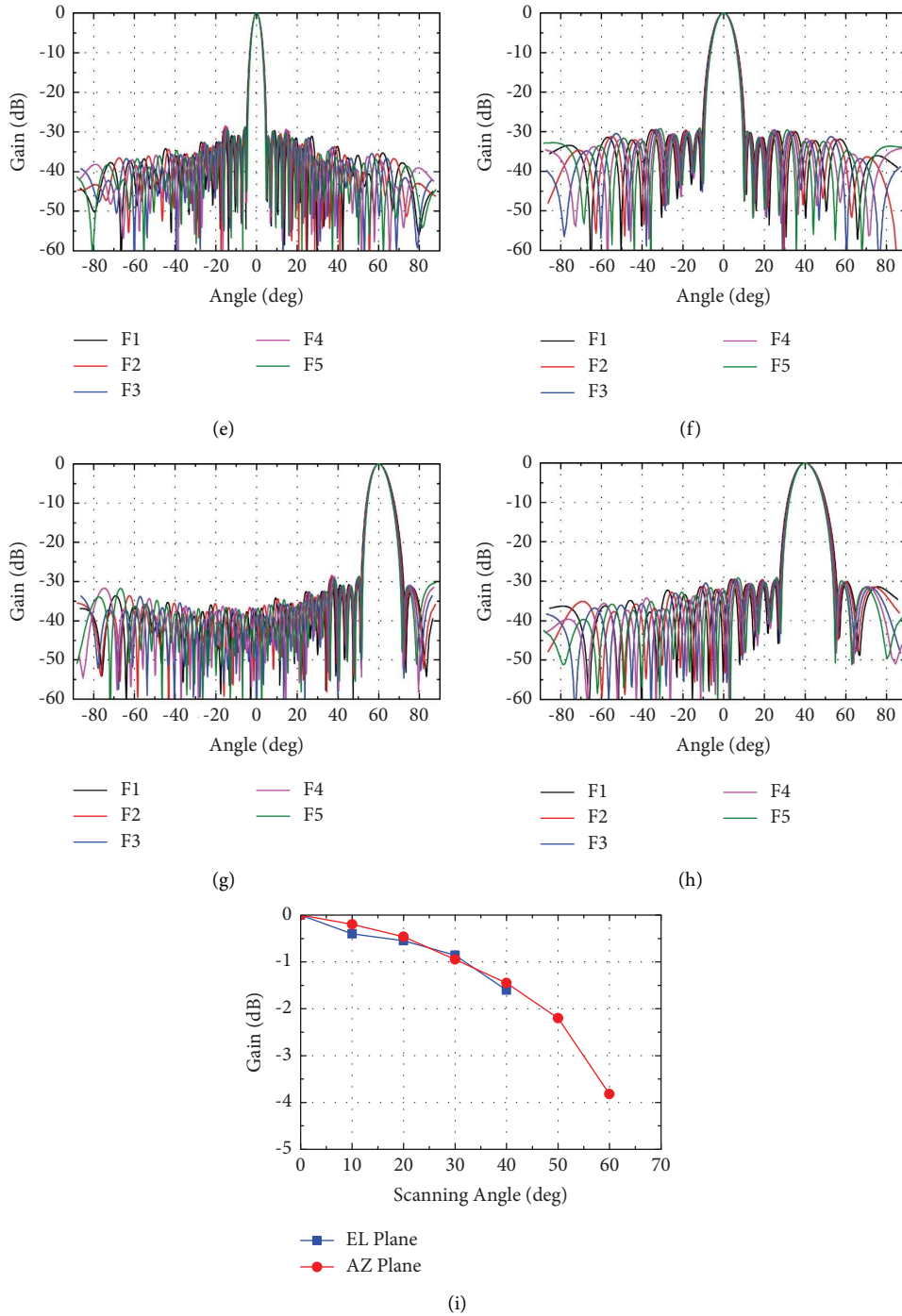


FIGURE 11: Wideband beam pattern. (a) Transmit 0° in azimuth plane. (b) Transmit 0° in elevation plane. (c) Transmit 60° in azimuth plane. (d) Transmit 40° in elevation plane. (e) Receive 0° in azimuth plane. (f) Receive 0° in elevation plane. (g) Receive 60° in azimuth plane. (h) Receive 40° in elevation plane. (i) Gain degradation with beam scanning.

far-field distance of about 100 meters, the residual frequency  $\Delta-k$  is approximately 0.17 MHz, as calculated using (16). It can be estimated that the beam pointing change is less than 0.01° when scanning up to 60° without compensating for this residual frequency. The experimental results in this paper

also show that this error does not affect the beam pointing accuracy. It can also be predicted that in practice, when the target distance estimation error is not greater than 500 meters, the pointing error caused by the residual delay in (16) is not greater than 0.03°, which is negligible.

## 6. Conclusion

In this paper, a wideband elemental digital array architecture based on the stretch processing method is proposed, and an antenna array prototype is developed and measured to verify the wideband performance of the array architecture. Compared to traditional wideband digital arrays, the stretch processing method can dramatically reduce the required sampling rate and lower the requirements on antenna hardware, thereby reducing the manufacturing cost of the system.

Based on the prototype, the cost is reduced over 75% after stretch processing. This architecture can be applied to various ground-based or vehicle-mounted radar systems with LFM waveform. The research is of great significance for the development of wideband phased array radar.

## Data Availability

The data used to support the findings of this study are available from the corresponding author upon request.

## Conflicts of Interest

The authors declare that they have no conflicts of interest.

## References

- [1] C. Tarran, "Advances in affordable digital array radar," in *Proceedings of the 2008 IET Waveform Diversity & Digital Radar Conference - Day 2: From Active Modules To Digital Radar*, pp. 1–6, London, UK, March 2008.
- [2] D. I. Voskresensky and E. M. Dobychnina, "Digital antenna array for multifunctional on-board radar," in *Proceedings of the 2011 21st International Crimean Conference Microwave & Telecommunication Technology*, pp. 525–526, Sevastopol, Ukraine, April 2011.
- [3] S. H. Talisa, K. W. O'Haver, T. M. Comberiate, M. D. Sharp, and O. F. Somerlock, "Benefits of digital phased array radars," *Proceedings of the IEEE*, vol. 104, no. 3, pp. 530–543, 2016.
- [4] C. Fulton, M. Yearly, D. Thompson, J. Lake, and A. Mitchell, "Digital phased arrays: challenges and opportunities," *Proceedings of the IEEE*, vol. 104, no. 3, pp. 487–503, 2016.
- [5] C. Ward, P. Hargrave, and J. McWhirter, "A novel algorithm and architecture for adaptive digital beamforming," *IEEE Transactions on Antennas and Propagation*, vol. 34, no. 3, pp. 338–346, 1986.
- [6] D. N. McQuiddy, R. L. Gassner, P. Hull, J. S. Mason, and J. M. Bedinger, "Transmit/receive module technology for X-band active array radar," *Proceedings of the IEEE*, vol. 79, no. 3, pp. 308–341, 1991.
- [7] R. J. Mailloux, *Electronically Scanned Arrays*, Morgan & Claypool, San Rafael, CA, USA, 2007.
- [8] R. J. Mailloux, *Phased Array Antenna Handbook*, Artech House, Norwood, MA, USA, 2005.
- [9] D. Pozar, *Microwave Engineering*, Wiley, Hoboken, NJ, USA, 2005.
- [10] T.-Do-Hong and P. Russer, "Signal processing for wideband array applications," *IEEE Microwave Magazine*, vol. 5, no. 1, pp. 57–67, 2004.
- [11] L. Huang, B. Shen, M. Li, and Z. Liu, "An efficient subband method for wideband adaptive beamforming," in *Proceedings of the 2008 10th International Conference on Advanced Communication Technology*, pp. 1489–1492, Gangwon, Korea, October 2008.
- [12] Schikorr, "High Range Resolution with digital stretch processing," in *Proceedings of the 2008 IEEE Radar Conference*, pp. 1–6, Rome, Italy, March 2008.
- [13] W. Fu and D. Jiang, "Radar wideband digital beamforming based on time delay and phase compensation," *International Journal of Electronics*, vol. 105, no. 7, pp. 1144–1158, 2018.
- [14] W. Fu, D. Jiang, Yu Su, R. Qian, and Y. Gao, "Implementation of wideband digital transmitting beamformer based on LFM waveforms," *IET Signal Processing*, vol. 11, no. 2, pp. 205–212, 2017.
- [15] W. J. Caputi, "Stretch: a time-transformation technique," *IEEE Transactions on Aerospace and Electronic Systems*, vol. 7, no. 2, pp. 269–278, 1971.
- [16] E. I. Brookner, *Radar Technology*, Dedham, Artech House, Massachusetts, MA, USA, 1977.
- [17] Z. De-ping, W. Chao, and N.-chang Yuan, "Design of transmit digital beam-forming system based on DDS array," *Modern Defense Technology*, vol. 39, no. 1, pp. 125–128, 2011.
- [18] L. H. Liu Haibo, E. Wang, L. J. Li Jinbing, and R. X. Ren Xiaoyuan, "Research on digital compensation technology of wideband phased array radar based on chirp signal," *IET International Radar Conference 2015*, pp. 1–5, 2015.
- [19] W. H. Weedon and R. D. Nunes, "Low-cost wideband digital receiver/exciter (DREX) technology enabling next-generation all-digital phased arrays," in *Proceedings of the 2016 IEEE International Symposium on Phased Array Systems and Technology (PAST)*, pp. 1–5, Waltham, MA, USA, March 2016.
- [20] Z. Liang, Q. Liu, and T. Long, "A novel subarray digital modulation technique for wideband phased array radar," *IEEE Transactions on Instrumentation and Measurement*, vol. 69, no. 10, pp. 7365–7376, 2020.
- [21] Y. Al-Alem, L. Albasha, and H. Mir, "High-resolution on-chip-band radar system using stretch processing-band radar system using stretch processing," *IEEE Sensors Journal*, vol. 16, no. 12, pp. 4749–4759, 2016.
- [22] M. Taghadosi, Y. Al-Alem, L. Albasha, and H. S. Mir, "Integrated stretch processed S-band digital radar system," in *Proceedings of the 2018 IEEE International Symposium on Circuits and Systems (ISCAS)*, pp. 1–5, Florence, Italy, September 2018.
- [23] A. J. Venere, S. Pazos, and M. Hurtado, "Low-cost high-resolution radar system using stretch processing," in *Proceedings of the 2022 IEEE Biennial Congress of Argentina (ARGENCON)*, pp. 1–6, San Juan, Argentina, May 2022.
- [24] M. M. Ashry, A. S. Mashaly, and B. I. Sheta, "Improved SAR range Doppler algorithm based on the stretch processing architecture," in *Proceedings of the 2022 International Telecommunications Conference (ITC-Egypt)*, pp. 1–6, Alexandria, Egypt, March 2022.
- [25] H. Malik, J. Burki, and M. Z. Mumtaz, "Adaptive pulse compression for sidelobes reduction in stretch processing based MIMO radars," *IEEE Access*, vol. 10, pp. 93231–93244, 2022.
- [26] L. C. Paul, M. I. Hasan, R. Azim, M. R. Islam, and M. T. Islam, "Design of high gain microstrip array antenna and beam steering for X band RADAR application," in *Proceedings of the 2020 Joint 9th International Conference On Informatics, Electronics & Vision (ICIEV) and 2020 4th International Conference On Imaging, Vision & Pattern Recognition (icIVPR)*, pp. 1–7, Kitakyushu, Japan, May 2020.

- [27] L. C. Paul, M. T. R. Jim, T. Rani et al., "A low-profile antenna with parasitic elements and a DGS-based partial ground plane for 5G/WMAN applications," *Discov Appl Sci*, vol. 6, no. 1, p. 22, 2024.
- [28] L. C. Paul, S. S. A. Ankan, T. Rani et al., "Design and characterization of a compact four-element microstrip array antenna for WiFi-5/6 routers," *International Journal of RF and Microwave Computer-Aided Engineering*, vol. 2023, pp. 1–13, 2023.
- [29] L. I. Ciociola, N. Ricciardella, R. Solimene, M. Felaco, and G. Pellegrini, "Digitally synthesized antenna test bench for next generation phased array systems," in *Proceedings of the 2022 IEEE International Symposium on Phased Array Systems & Technology (PAST)*, pp. 1–6, Waltham, MA, USA, March 2022.